

1994 NASA/ASEE SUMMER FACULTY FELLOWSHIP PROGRAM

111 762

JOHN F. KENNEDY SPACE CENTER
UNIVERSITY OF CENTRAL FLORIDA

511-37

33971

p. 26

DESIGN OPTIMIZATION OF A BRUSH TURBINE
WITH A CLEANER/WATER BASED SOLUTION

PREPARED BY:	Dr. Rhyn H. Kim
ACADEMIC RANK:	Professor
UNIVERSITY AND DEPARTMENT:	University of North Carolina at Charlotte Department of Mechanical Engineering and Engineering Science
NASA/KSC	
DIVISION:	Mechanical Engineering
BRANCH:	Special Projects
NASA COLLEAGUE:	Rudy Werlink
DATE:	August 5, 1994
CONTRACT NUMBER:	University of Central Florida NASA-NGT-60002 Supplement: 17



ABSTRACT

Recently, a fluid turbine which has a brush attached to it has been designed and tested with water as fluid. The purpose of the turbine-brush is to clean up fouling in a tube. The Montreal Protocol prohibits the use of CFC products from refrigeration industry or from industry in general as a cleanser in 1996. Alternatives for the cleansers, devices or a combination of alternative devices with a cleanser should be found. One of the methods is to develop a device which cleanses fouling with a cleaning medium. In this paper, we describe a turbine connected with a brush. However, the turbine with the brush should be simple and easy to install. This device is a combined small liquid turbine with a brush. The turbine is activated by the liquid flowing through the tube. Then the turbine turns the brush cleaning fouling along the tube. Based on the energy conservation and the Bernoulli equation along with an empirical relationship of drag force obtained from an experimental apparatus, a relationship of the rotational speed, the number of blades, and geometric variables of the turbine-brush was obtained. The predicted rotational speeds were compared with the experimental observations. Further work was recommended for improvements.

SUMMARY

One of methods of cleaning fouling in a tube will be a turbine-brush unit to replace R113 as a cleanser after 1995. The turbine-brush consists of a turbine and a brush with a connector between the two. The turbine-brush was created in KSC, NASA and demonstrated its rotational motion while it was held at a position.

Objective of the program is to optimize the geometry of the turbine-brush including the blade angle, the number of blades, and arrangements of the connector and brush, flow rates, rotational speeds, diameters of tubing and performance of cleaning before a final product is designed and manufactured.

As an initial step, a relationship among the above variables was developed based on the energy conservation law and the force momentum theorem. Numerical values of an existing turbine-brush are used with the relationship to predict the rotational speed. Predicted rotational speeds are compared with observed rotational speeds. These two differ in one order of magnitude.

The drag coefficients were computed based on the incoming velocity. From the open literature, we did not find any information of its drag force coefficients, because this may be the first device to do the cleaning in the tube with the fluid as driving energy source. Possible alternative coefficients useable for the turbine-brush are those for a spinning sphere or a disk and cylinder connected in tandem. From the experimental results, the force was measured and its coefficient was calculated. As a result, the equation relating the variables produced the angular velocity.

While it rotates, the flow downstream of the turbine-brush is a combination of a usual turbulent one dimensional flow with a forced vortex motion due to the turbine motion within the connector and brush then one more complicated form of forced vortex motion takes place downstream of the brush. A laminar sublayer flow was assumed to pass through the gap between the turbine-brush and the wall of the tubing.

A simple numerical model was developed. One hundred sixty eight volume elements were constructed in order to use in a three dimensional unsteady flow conditions. Boundary conditions, properties, turbulence model, and so on have to be supplied to run and yield a result.

Further work is recommended as follows: (1) a coded program of computation is recommended for various parameters of the turbine-brush, (2) measurement of drag force coefficients in the wide range of the volume rates, (3) study of constraints under which the relationship derived be optimized including the degree of the reaction of the turbine, (4) experiments be performed with a different forms of the brush, (5) a numerical simulation be continued with the model to determine a feasibility of the numerical scheme for the turbine-brush in the future.

TABLE OF CONTENTS

Section	Title	Page
	Cover/Title Page	
	Abstract	
	Summary	
	List of Figures	
	Nomenclature	
I	INTRODUCTION	
II	ANALYSIS	
2.1	Drag Force and its Coefficient	
2.2	Energy Conservation Law	
2.3	Application of the Derived Equation	
2.4	Numerical Simulation	
III	EXPERIMENTAL INVESTIGATION	
3.1	Type of Probes and Their Locations	
3.2	Data from Experiments and Computed V_1, C_D	
IV	RESULTS AND DISCUSSIONS	
4.1	Angular Velocity and frequency	
4.2	Coefficients of Drag Forces	
4.3	Constraints under Which Optimum Values Are Obtained	
4.4	Numerical Simulation	
V	RECOMMENDATION	
VI	CONCLUDING REMARKS	
VII	APPENDIX	
	A DERIVATION OF KINETIC ENERGY OF ROTATING ELEMENTS	
	B DERIVATION OF ROTATIONAL WORK DUE TO CENTRIFUGAL FORCE	
	C THE NEWTON-RAPHSON METHOD FOR FINDING ROOTS OF A POLYNOMIAL	
VIII	REFERENCES	

LIST OF FIGURES

- Fig.1 Dimensions of Turbine-Brush
- Fig.2 Control Volume and a Schematic Diagram of a Turbine-Brush Unit
- Fig.3 Finite Volume Element Structure
- Fig.4 Experimental Apparatus and Probe Locations
- Fig.5 Inlet and Exit Vector Diagram and Combined Vector Diagram
- Fig.6 Mass Moment of Inertia, Centrifugal Force Friction Force
- Fig.7 Radii of Turbine-Brush, (a) Turbine and its Housing, (b) Connector, (c) Brush

NOMENCLATURE

A	Area of tube cross-section, m^2
B	Width of the brush, or the length of turbine-brush sections, m
C_D	Drag coefficient
d	Diameter of the tube, m
F	Force, N
g_c	Constant defined by the force:unity is the SI unit
H	Enthalpy, kJ/s
h	specific enthalpy, kJ/kg
K.E.	Kinetic energy, kJ/kg
m_r	Mass rate, kg/s
p	Static pressure, N/m^2
P.E.	Potential energy, kJ/kg
Q	Heat transfer rate, J/s
r	radii of the rotating elements, m
u	Specific internal energy, kJ/kg
U	Tangential Velocity, m/s
V	Fluid velocity, m/s
v	Specific volume, m^3/kg
W	Rate of work, kJ/s

Greek Letters

α	Turbine angle
β	Weight adjusting factor
π	3.14
ρ	Density, kg/m^3
Σ	Summation
ω	Angular velocity, /s
μ	Dynamic viscosity, $N s/m^2$

Subscripts

1-2	representing the length between p_1 and p_2
1-4	representing the length between p_1 and p_2
b.b.	Brush Base
b.h.	brush and its hub
br	Brush
D	Drag force
f	Fluid
in	Entering section
out	exiting section
shaft	shaft work
skin.f.	Shear force
rot.	Referring to rotational parameters
tension	Tension of a wire
tur	turbine

I. INTRODUCTION

CFC refrigerants/cleaners will not be allowed to use in cleaning fouling in tubes starting in 1996. In this paper, we describe a device which will clean fouling in tubes. The device consists of two parts; a turbine and a brush with a connecting part. Details of the turbine, brush and the connector are shown in Fig.1(Werlink,1993). The turbine has four blades with 70 degree wide and there is a spacing of 20 degrees between the blades. These blades are installed in a direction of 45 degree from the axial direction. A connector links the turbine with a brush.

The brush is made of nylon fibers so very densely structured that fluid may not pass through. It is possible to consider that the friction in the gap between the turbine and the tube wall and brush and wall may be of a nature of a laminar flow. However, the drag force of the turbine-brush unit is very complicated. At a glance, the unit may be assumed to be a spinning sphere(Goldstein) or a disk connected to a cylinder in tandem(Blevins). While a cleanser water solution passes through a tube, more or less, the friction force may be reduced due to the fact that the cleanser is a material made of long chain structured polymers(Sellin and Moses). On the other hand, a constant vortex motion provided by the turbine followed by a swirling motion of the fluid within the connector and the brush, again, a vortex motion due to the brush rotation are very complicated and difficult to analyze exactly.

The combined vortex and turbulent flow may be analyzed by superimposing two separate flow characteristics together, i.e., an axial turbulent flow passing through the geometry of the turbine-brush and a rotational flow within the turbine-brush configuration may be analyzed separately and results should be superimposed.

In this project, preliminary results were obtained based on simplifying assumptions and measurements of drag forces. Based on the assumptions, the energy conservation law was used along with the force momentum theorem tying up with the drag force in terms of pressure drops across the turbine-brush. By doing so, the speed of the unit in rotational motion was predicted and compared with the experimental results.

II. ANALYSIS

2.1 Drag Force and its Coefficient

Consider a control volume shown in Fig.2. Certain assumptions are needed to deal with the flow phenomena for a first order approximation solution. The assumptions used for the fluid

are(Munson et al.):

1. One-dimensional incompressible steady flow
2. No heat transfer from or to the flow, and $t_{in} = t_{out}$.
3. Fully developed turbulent flow
4. The tube has a uniform internal diameter.
5. The fluid has constant dynamic and thermal properties.
6. Fluid passing through the brush section is a negligible amount.
7. The drag force of the turbine-brush held at a position will be the same as it moves, once the tension force is taken into account in computing the drag coefficient.

Based on the force-momentum theorem, the sum of forces in the horizontal direction is the same as the rate of momentum change(Munson, et.al):

$$\Sigma F = (m_f/g_c)(V_{out} - V_{in}) \quad (1)$$

The sum of forces are collection of the tension force, static forces, the drag force and the skin friction forces(Fig.2):

$$- F_{tension} + (p_1 - p_2)A + F_D - F_{skin.f.1-2} = (m_f/g_c)(V_2 - V_1) \quad (2)$$

where p's are the static pressures measured at the upstream and downstream of the turbine-brush. If the static pressures at the stations 1 and 4 are used equation(2) becomes(Fig.4):

$$-F_{tension} + (p_1 - p_4)A + F_D + F_{skin.f.1-4} = (m_f/g_c)(V_4 - V_1) = 0$$

because V_4 is the same as V_1 for a fully developed flow at the station 4 in the tube. From the above, we obtain F_D :

$$F_D = F_{tension} + (p_4 - p_1)A - F_{skin.f.1-4}$$

By the definition of the drag coefficient, C_D , the drag force is given by:

$$F_D = \rho_f V_1^2 A C_D / (2g_c)$$

$$C_D = [F_{tension} + (p_4 - p_1)A - F_{skin.f.1-4}] / (\rho_f V_1^2 A / 2g_c) \quad (3)$$

The coefficient, C_D is computed from equation(3) with $F_{tension}$, p_4 , p_1 , and V_1 which come from experiments. The skin friction force is in terms of viscosity, the velocity gradient at the laminar sublayer in the gap between the turbine and tube wall and the brush and tubing wall. The friction force in the axial direction has a form:

$$F_{skin.f.1-4} = \mu_f V_1 (2\pi B_{1-4}) \quad (4)$$

2.2 Energy Conservation Law

Consider the energy conservation on the control volume shown in Fig.2(Moran and Shapiro):

$$Q - W = (K.E. + P.E. + H)_{out} - (K.E. + P.E. + H)_{in} \quad (5)$$

where Q is the heat transfer rate, W , the mechanical work and K.E. and P.E. are the kinetic and potential energy, respectively and H is enthalpy defined by:

$$H = m_f h; \quad h = u + p/\rho, \quad m_f = \text{mass rate} \quad (6)$$

Applying the usual assumptions to liquid steady flows, i.e., no heat transfer, temperature being unchanged, i.e., $t_{in} = t_{out}$, and the density being constant, the above equation is written as follows:

$$-W = (m_f/g_c)[(V_2^2/2 + p_2 v) - (V_1^2/2 - p_1 v)] \quad (7)$$

The rate of work in equation(7) includes the shaft work and the friction work as the unit rotates:

$$W = W_{shaft} + W_{skin.f.} \quad (8)$$

Since the rotational force comes from the motion of the blades, all of energy of fluid is assumed to turn the turbine-brush, the shaft work will have a form:

$$W_{shaft} = J_{tot} \omega^2 / 2 \quad (9)$$

where ω is the angular velocity and J_{tot} is the sum of the moment of inertia about the axial direction. The sum of the moments consists of moments of inertia of the turbine, J_{tur} , the connectors, $J_{conn.}$, brush hub, $J_{b.h.}$ and the brush, J_b .

$$J_{tur} = (\rho t)_{tur} (\pi/2) (r_4^4 - r_1^4) (\alpha/360) N \beta_{tur} \quad (10)$$

$$J_{conn.} = (\rho t)_{conn.} (\pi/2) (r_3^4 - r_2^4) \beta_{conn.} \quad (11)$$

$$J_{b.h.} = (\rho B)_{b.h.} (\pi/2) (r_3^4 - r_2^4)_{b.h.} \quad (12)$$

$$J_b = (\rho B)_b (\pi/2) (r_3^4 - r_2^4)_b \quad (13)$$

where ρ is the density, t is the thickness, α is the angle of the blade, and β is a number adjusting the geometry with respect to one of the components of the turbine-brush, N , the number of blades, and r 's are radii, respectively (See details in derivations of APPENDIX).

Since the turbine-brush unit is held in a position but rotates, the friction work due to the translation motion is negligible. The friction between the brush and surface of the tube wall is due to the force normal to the centrifugal force. This force should be multiplied by the tangential velocity of rotation (See details in derivation of APPENDIX):

$$W_{br,rot} = (2\pi/3g_c)\mu_{dry}(\rho B)_{br}\omega^3 r_7(r_7^3 - r_2^3)_{br}\beta_{b.h.} \quad (14)$$

The magnitude of the dry friction coefficient between the turbine the brush and the tube wall is 0.35 (Baumeister and others). Since the flow in the gap between the tube wall and turbine housing is laminar, the work against the rotational motion is:

$$W_{rot.} = (2\pi/3g_c)\mu_f(\rho B)_{tur}\omega^3 N r_4(r_4^3 - r_1^3)_{tur}\beta_{tur} \quad (15)$$

After collecting all of these terms, equations (2), (3), (4), (9-15) and substituting into equation (7), a relationship of important variables such as the angular velocity, the speed of the unit along the tube, and the number of the blades is shown as follows.

$$\begin{aligned} c_1 r_7(r_7^3 - r_3^3)\omega^3 + c_2 r_4(r_4^3 - r_1^3)N\omega^3 - c_3(r_4^4 - r_1^4)N\omega^2 - \\ (c_4 + c_5)(r_3^4 - r_2^4)\omega^2 - c_6(r_7^4 - r_3^4)\omega^2 \\ + c_7(r_6 + r_1)^2\omega^2 - c_8 = 0 \end{aligned} \quad (16)$$

where

$$c_1 = (2\pi/3g_c)\mu_{dry}(\rho B)_{br}\beta_{b.h.} \quad (17a)$$

$$c_2 = (2\pi/3g_c)\mu_f(\rho B)_{tur}\beta_{tur}(\alpha/360) \quad (17b)$$

$$c_3 = (\pi/2)(\rho B)_{tur}\beta_{tur}(\alpha/360)/2g_c \quad (17c)$$

$$c_4 = (\pi/2)(\rho t)_{conn.}\beta_{conn.}/2g_c \quad (17d)$$

$$c_5 = (\pi/2)(\rho B)_{b.h.}/2g_c \quad (17e)$$

$$c_6 = (\pi/2)(\rho B)_b/2g_c \quad (17f)$$

$$c_7 = m_f/(8g_c) \quad (17g)$$

$$c_8 = - (m_f/2g_c)V_1^2 C_D + F_{tension}V_1 \quad (17h)$$

where $\beta_{b.h.}$ is a factor adjusting the geometry for the brush and hub, $\beta_{conn.}$, a factor adjusting the geometry for the connector, and β_{tur} is a factor adjusting the geometry for the turbine. $V_2^2 = V_{2trans.}^2 + V_{2rot.}^2$, $V_1^2 \approx V_{2trans.}^2$ $V_{2rot.} = ((r_6 + r_1)/2)\omega$ were also used in equation(16). Subscripts 1, and 2, here refer to the inlet and outlet, respectively.

2.3 Application of the Derived Equation

For the number of blades, $N= 4$, r 's being read from Fig.1, listed in Table 1, equation(16) becomes a third degree polynomial in ω at a given volume rate, .i.e., $V_1 = \text{constant}$:

$$a_3\omega^3 + a_2\omega^2 - a_0 = 0 \quad (18)$$

where a 's are expressed as follows:

$$a_3 = c_1r_7(r_7^3 - r_3^3) + c_2r_4(r_4^3 - r_1^3)N \quad (19a)$$

$$a_2 = c_7(r_6 + r_1)^2 - [c_3N(r_4^4 - r_1^4) + (c_4 + c_5)(r_3^4 - r_2^4) + c_6(r_7^4 - r_3^4)] \quad (19b)$$

$$a_0 = c_8 \quad (19c)$$

where C_p is assumed to depend on the incoming velocity, V_1 and constant determined from the experiments. Table 1 summarizes all of the numbers in the above computations.

Table 1 Values of material properties, geometry and flow properties

Turbine	Brush	Brush Hub	Connector
$r_1=0.00381\text{m}$	$r_2=0.00508$ $r_3=0.00762$	$r_2=0.00508$ $r_3=0.00762$	$r_2=0.00508$ $r_3=0.00762$
$r_4=0.01905$ $r_5=0.02159 \text{ m}$ $r_6=0.02301 \text{ m}$ $r_7=0.0254 \text{ m}$ $t=0.0015875 \text{ m}$	$r_7=0.0254 \text{ m}$		$t=0.0015875$
$B=0.0047625 \text{ m}$	$B=0.008382 \text{ m}$	$B=0.008382 \text{ m}$	$B=0.00254$
$\rho=7900 \text{ kg/m}^3$	$\rho=1121.625 \text{ kg/m}^3$	$\rho=4800 \text{ kg/m}^3$	$\rho=7900 \text{ kg/m}^3$

The density and viscosity of fluid are $\rho=997 \text{ kg/m}^3$ and $\mu=885 \times 10^{-6} \text{ Ns/m}^2$.

2.4 Numerical Simulation

A software NEKTON(Fluent,Inc.) was made available on a DEC workstation in the Branch through the KSC Telnet network. NEKTON is a finite element based fluid problem solver that is capable of analyzing flows of three dimensional unsteady nature. This is a result of a spectral element method developed by Professor Patera of MIT and commercialized by Fluent,Inc.

The flow domain of the turbine-brush is a cylinder with a length of $11d$, d being the diameter of the cylinder. At the location of $3d$ from the entrance, the turbine-brush of $2d$ long is placed. The location of the exit is then $6d$ away downstream from the turbine-brush which may be the minimum distance for which a fully developed flow at the exit is warranted.

Starting from the entrance, 21 surface elements were constructed. These elements were moved up to the next position along the cylinder length, thereby, became volume elements. At the location of the turbine brush, the surface was divided into different concentric elements from the previous fluid elements so that these elements are identified as rotating elements at given locations. The connector and brush sections were made into volume elements in a similar manner to the turbine section(Fig.3).

At present, 168 finite volume elements were constructed for the flow domain and stored in the SUN workstation network at UNC-Charlotte. Additional variables to be supplied are boundary conditions, fluid properties, rotating boundary conditions, turbulence model, and deformation information for each element. This is a very crude model for the turbine-brush. However, this would yield important an insight so that an analyzer can determine whether a numerical study may be of help in the turbine-brush development.

III.EXPERIMENTAL INVESTIGATION

3.1 Type of Probes and Their Locations

Fig.4 shows an experimental apparatus. A hydrant with a control valve supplies water to the test section of a transparent tubing of i.d., 2 in. The valve controls the flow rate. The turbine-brush unit is held by a wire and a load cell transducer measures the tension force of the wire. The pressure ports are shown as p_1 , p_2 , p_3 , and p_4 . The rotation speed was measured by picking up pulses from a

rotating magnet which is placed in a turbine blade. The sampling rate was 49.98 per second. The load cell and pressure transducers have the measuring ranges as shown in Table 2.

Table 2 Transducer Ranges

Transducers	ranges	Accuracy in F.S.
Load cell	0-50 lb	0.1 %
P ₁	14.7-60 psia	0.02%
P ₂	14.7 - 50psia	0.02%
P ₃	12.0 - 30psia	0.02%
P ₄	12-30 psia	0.02%

A PC and labview software display and record the data in an ASCII file in a monitor and disk. A typical data set is shown in Table 3.

3.2 Data from Experiments and V₁, F_D Computation

Applying the force-momentum theorem to the turbine-brush held at a point produces an equation in the form:

$$-F_{\text{tension}} + (p_1 - p_2)A + F_{\text{Drag}} - F_{\text{skin.f.1-2}} = (m_f/g_c)(V_2 - V_1) \quad (2)$$

where the first two quantities of the left hand side of the equality and V₁ are known and the drag force is given by $F_{\text{Drag}} = C_D \rho_f V_1^2 A / 2g_c$, A being the cross section area of the tube. From this equation V₂ is obtained. Computation yielded that V₂'s are within a range of 95 percent of V₁. Table 3 summarizes data from the experiments, computed velocities and the drag forces. The quantities in parentheses are the numbers in the Pound-Inch system.

The reading devices have ranges of uncertainties within 0.10 percent, yielding an uncertainty of about 1.0 percent for the measurement system.

Table 3 Summary of Flow Rates, Pressures, Tension Force and Drag Force

Flow Rate	p_1	p_2	p_3	p_4	$F_{tension}$	V_1	Drag Force
m^3/s (gpm)	kpa (psi)	kpa (psi)	kpa (psi)	kpa (psi)	N (lbs)	m/s (ft/s)	N (lbs)
.0037 (58.5)	21.86 (3.17)	10.34 (1.50)	1.014 (0.147)	2.64 (0.38)	39.44 (8.86)	1.822 (5.98)	0.468 (.105)
.0047 (74.47)	21.79 (3.16)	10.76 (1.56)	1.048 (0.152)	2.64 (0.38)	41.15 (9.25)	2.32 (7.61)	0.53 (2.36)
.0052 (82.00)	20.80 (3.02)	10.74 (1.60)	1.50 (0.218)	2.81 (0.41)	39.41 (8.86)	2.01 (6.58)	0.655 (2.97)

IV. RESULTS AND DISCUSSION

4.1 The Angular Velocity

In the computation procedure, the geometry factors were used; $\beta_{b.h.} = 72$, $\beta_{conn.} = 72$, and $\beta_{tur} = 0.65$. Table 4 shows the computed and observed frequencies for three cases. The predicted and the observed frequencies do not agree well. The predicted values are of magnitude of one order higher than the observed values. This means that the mass of the rotating system has been estimated less than it should be and that the sum of the inertia of rotating parts of the turbine-brush should be estimated more carefully, rather than using the geometry factors.

One of the assumptions used was the flow in the gap between the turbine-brush and the tube wall is a laminar sublayer. This may not be true. Estimating the frictional work in the rotating motion of the turbine-brush may not be accurate, particularly with the brush. More data are needed for the drag coefficients in a wide range of the volume rates to know whether the deviation between the two values of the angular velocities would be greater in the high Reynolds number side.

4.2. Coefficients of Drag Forces

From Table 3, the drag coefficients were computed for three different flow rates. The Reynolds numbers and the coefficients are listed in Table 4. Further computed results will be compiled for a later report.

Table 4 Coefficients of Drag forces at Flow Rates

Flow Rate m ³ /s (gpm)	Re	C _D	f _{pred.}	f _{observed}
0.0037(58.5)	1.08x10 ⁵	0.14	43.98	7.0
0.0047(74.47)	1.37x10 ⁵	0.43	47.41	7.0
0.0052(82.00)	1.19x10 ⁵	0.20	47.86	7.0

The difference between the incoming velocity and the moving speed of the turbine-brush is very little. The drag coefficient changes from 0.14 to 0.4 in the Reynolds number range at 10⁵. The coefficient of the turbine-brush is compared to those of the spinning sphere(Goldstein), and the disk connected to a cylinder in tandem. The drag coefficients of the turbine-brush is less than the spinning sphere and the disk connected to a cylinder(Blevins).

4.3 Constraints under which optimum values are obtained

An important constraint among others seems to be the degree of the reaction of the turbine-brush, which is defined as(Shepherd):

$$R = [(U_1^2 - U_2^2) + (V_{r2}^2 - V_{r1}^2)] / (2g_c E) \quad (20)$$

where E is defined as:

$$E = [(V^2 - V_2^2) + (U_1^2 - U_2^2) + (V_{r2}^2 - V_{r1}^2)] / (2g_c) \quad (21)$$

where all of the symbols used are denoted in Fig.5. The absolute velocity V is resolved into a component V_m passing through the axis(a radial velocity) and a tangential component V_u. The reaction is an indication of energy transfer from the fluid to the turbine. For example, R = 0 implies that there is no change of static head or pressure in the rotor and such a machine is called an impulse type. In general, the term reaction alone is used whenever the turbine is not purely impulse, but for the special case of steam turbines, it has come to imply 50 percent or half degree of the reaction. The turbine of the turbine-brush has a degree of the reaction between 0 and 50 percent. This aspect of the degree of reaction for the turbine-brush should be studied further.

Other important constraints are the optimum radii of the structure because these determine the weight of the turbine-brush, consequently the rotating inertia. The structure of the connector seems to be a very important constraint. A new arrangement and structure of the brush will be important. All of these variables are related with the geometry factors. The more accurate these are, the better predictions seem to be made.

Strictly speaking, the actual application of this device in cleaning fouling, the device will travel along the tube, not held at a place. The current experimental apparatus holds the turbine-brush at a point, thus the drag coefficient might be different from those obtained from the apparatus in which the turbine-brush was held at a point. A series of this type of experiments should be carried out in the future.

4.4 Numerical Simulation

The numerical analysis be continued to establish a feasibility study. This type of the feasibility study may be needed to justify the required time for a coding a new program or justify using a commercially available code, if needed.

V. RECOMMENDATION

Further work is recommended as follows.

1. Determine the weights of the turbine-brush as a unit and individual components. This will help determine the mass moment of inertia of the turbine-brush and mass adjusting factors, because these control the prediction of the rotation speed.
2. More drag force measurements may be needed from low volume rates. Additional experiments would tell us whether the prediction is reliable in the low or high velocity side of the flows.
3. Investigation of the constraints under which the relationship derived be optimized including the degree of the reaction of the turbine. Because of the brush attached to the turbine, this may be a brand new study.
4. Different forms of brushes be attached and experimented for a possible reduction of the drag force. Rather than the radial brush, attach fibers in the connector along the axial direction so that the fibers get stretched due to the centrifugal force in rotation. This would reduce the drag force and enhance the rotational speeds. This kind of fiber arrangement could be beneficial for a smaller diameter.

5. Computation procedures be coded for the current verification of the equation as well as its future use.

6. Numerical analysis with constructed elements be carried out to determine feasibility for further numerical study and to know whether it could aid the design development activity based on the software NEKTON or a different code or coding a new code.

VI. CONCLUDING REMARKS

Based on the Newton's law of force and the energy conservation law, an equation was derived relating certain number of geometrical variables with flow variables together. Pressure drops across the turbine-brush were measured in order to compute the drag force coefficients. These coefficients were used in the derived equation. This equation provided the rotations per second. These have been compared with the experimental values. They do not agree at all. The reason was discussed in the Results and Discussion section. Further work has been suggested in the Recommendation section.

VII. APPENDIX

A. DERIVATION OF THE KINETIC ENERGY OF THE BLADES

From Figs. 6(a) and 7(a), the mass moment of inertia of the arc element is:

$$dI = r^2(dm); \quad dm = \rho(2\pi r dr)t = 2\pi(\rho t)r dr; \quad dI = 2\pi(\rho t)r^3 dr$$

$$I = \int 2\pi(\rho t/g_c)r^3 dr = (\pi/2g_c)(\rho t)(r_2^4 - r_1^4) \quad (A1)$$

where ρ is the density, and t is the thickness of a plate.

Integration of the above with respect to the radius for a blade that has α degree, the outer and inner radii as r_2 and r_1 gives:

$$I_{tur} = (\pi/2g_c)(\rho t)_{tur}(r_2^4 - r_1^4)(\alpha/360) \quad (A2)$$

Thus, the kinetic energy of the N turbine blade is:

$$(\pi/2g_c)(\rho t)_{tur}\omega^2(r_2^4 - r_1^4)N/2 \quad (A3)$$

B. DERIVATION OF THE OF THE ROTATIONAL FRICTIONAL FORCE AND ITS WORK

From Figs. 6(a) and 7(b), the centrifugal force of the arc element is:

$$dF_{cent} = r\omega^2(dm); \quad dm = \rho(2\pi r dr)B; \quad \omega = \text{constant} \quad (B1)$$

where ω is the angular velocity of the blade. Integration of the force with respect to the blade angle and radius with the number of blades gives:

$$F_{cent} = (2\pi/3g_c)(\rho t)_{tur}\omega^2(r_4^3 - r_1^3)(\alpha/360)N \quad (B2)$$

The friction force is, then:

$$F_{frict} = \mu_{dry}F_{cent},$$

where μ_{dry} is the dry friction coefficient between the brush and the tube wall. Thus, the rate of the frictional work is:

$$W_{br,rot} = (2\pi/3g_c)\mu_{dry}(\rho B)_{br}\omega^3r_2(r_7^3 - r_2^3) \quad (B3)$$

C. THE NEWTON-RAPHSON METHOD FOR FINDING ROOTS OF A POLYNOMIAL

Consider a function of x , $f(x) = a_0 + a_1x + a_2x^2$

$$+ a_3x^3 + a_4x^4 + \dots \quad (C1)$$

Suppose an estimated root is x_0 . Then evaluate the function $f(x_0)$, that is:

$$f(x_0) = a_0 + a_1x_0 + a_2x_0^2 + a_3x_0^3 + a_4x_0^4 + \dots \quad (C2)$$

Take the derivative of the function with respect to x and substitute x with x_0 :

$$df(x_0)/dx_0 = a_1 + 2a_2x_0 + 3a_3x_0^2 + 4a_4x_0^3 + \dots \quad (C3)$$

Now make a ratio of $f(x_0)/df(x_0)/dx$, subtract from x_0 and set it as:

$$x_n = x_0 - f(x_0)/df(x_0)/dx \quad (C4)$$

Let us compare x_n with x_0 in terms of their magnitudes; hence the absolute value of the difference is less than a certain number, $\varepsilon = 0.01$ for which the accuracy is warranted:

$$|x_n - x_0| \leq \varepsilon \quad (C5)$$

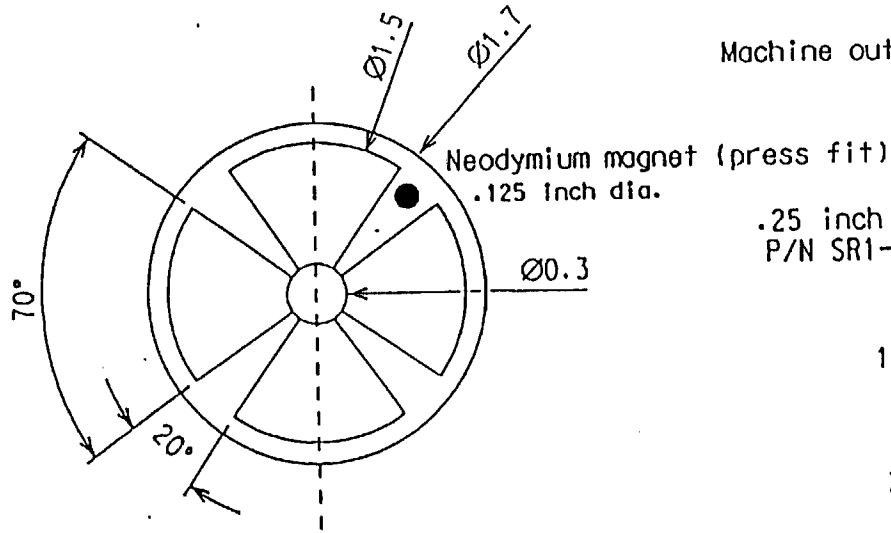
then, one of the roots of equation(8) is x_n . For other roots, the above procedure should be repeated for the polynomial(Stoecker).

Using velocities of Table 3 and C_D 's of Table 4 for three cases of experimental results, the roots were found. $\omega = 276.2072, 297.7274,$ and $300.5572,$ respectively. The other two roots are imaginary numbers for the three cases. Thus $\omega = 2\pi(\text{rotation/s})$ produces $43.98, 47.41,$ and 47.86 for rotations per second, which is frequency.

VIII. REFERENCES

1. Werlink, R., Private Communication on Patent Application, KSC, NASA, Nov., 1993, May, 1994
2. Goldstein, S., Modern Developments in Fluid Dynamics, Oxford Press, London, 1938
3. Blevins, R., Advanced Fluid Dynamics Handbook, Van Nostrand Reinhold, New York, 1984, p.333
4. Sellin, R.H., Moses, R.T., Drag Reduction in Fluid Flows, Techniques from Friction Control, Ed. Ellis Horwood limited, 1989
5. Munson, B.R., Young, D.F., Okiishi, T.H., Fundamentals of Fluid Mechanics, 2nd Ed. John-Wiley & Sons, Inc., 1994
6. Moran, M.J., Shapiro, M.J., Fundamentals of Engineering Thermodynamics, 2nd Ed., John-Wiley & Sons, Inc., New York, 1992
7. Baumeister, T., Avallone, E.A., and Baumeister, T, III, Marks' Handbook of Mechanical Engineers, 8th Ed., McGraw-Hill Book co., 1978
8. Fluent Inc., NEKTON, Ver. 2.85, User's Guide, Lebanon, N.H., 1992
9. Shepherd, D.G., Principles of Turbomachinery, Macmillan Co., 1969
10. Stoecker, W.F., Design of Thermal Systems, McGraw-Hill Book Co., 1971

Top view of Ring (no blades)



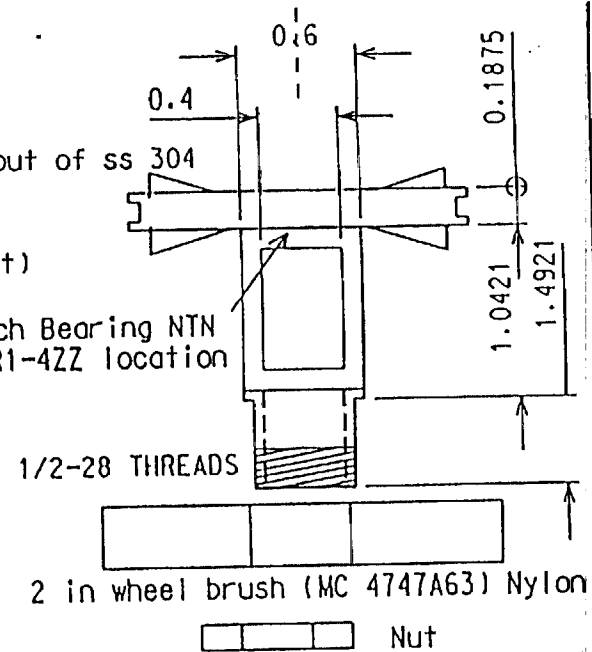
Machine out of ss 304

.25 inch Bearing NTN
P/N SR1-4ZZ location

1/2-28 THREADS

2 in wheel brush (MC 4747A63) Nylon

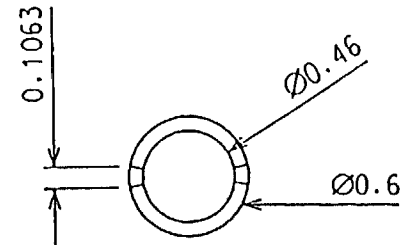
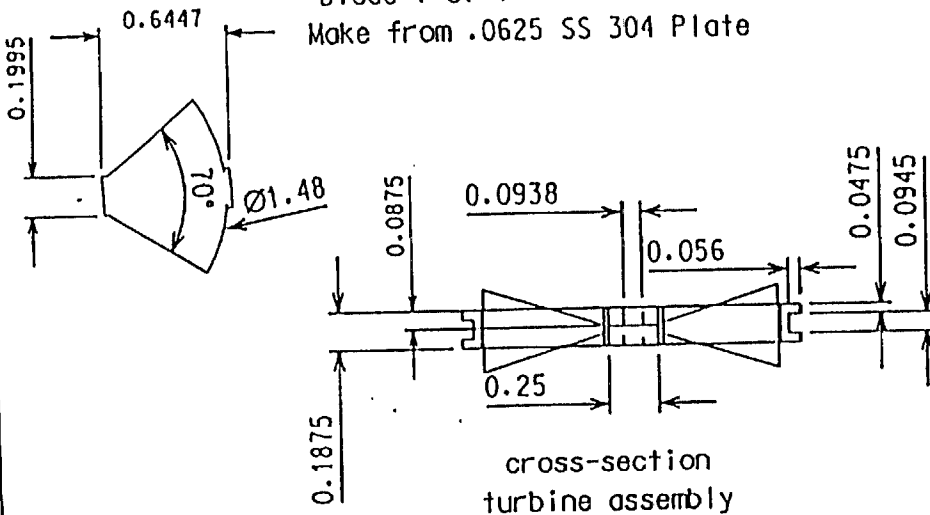
Nut



silver solder to ring and hub at 45 deg angle from horizontal edge

Blade 1 of 4

Make from .0625 SS 304 Plate



standoff (top view sliced)

scale=1 inch

Rudy werlink DM-MED-11

Fig.1 Dimensions of Turbine-Brush

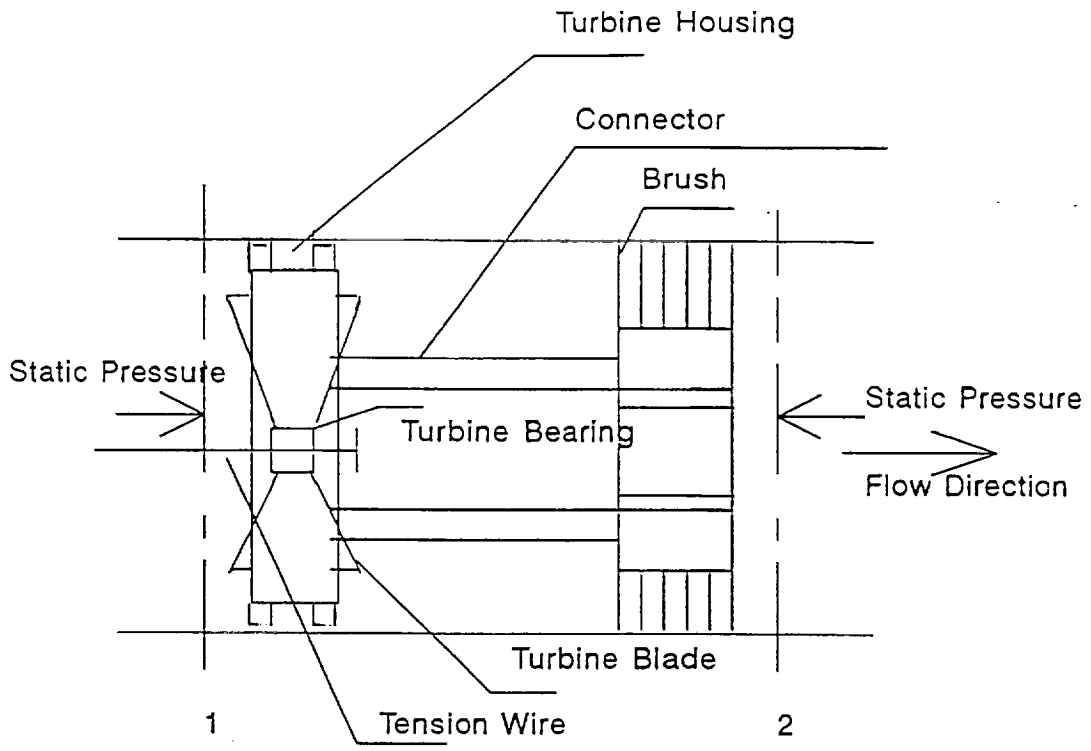


Fig.2 A Control Voume and a Schematic Diagram of a Turbine-Brush Unit

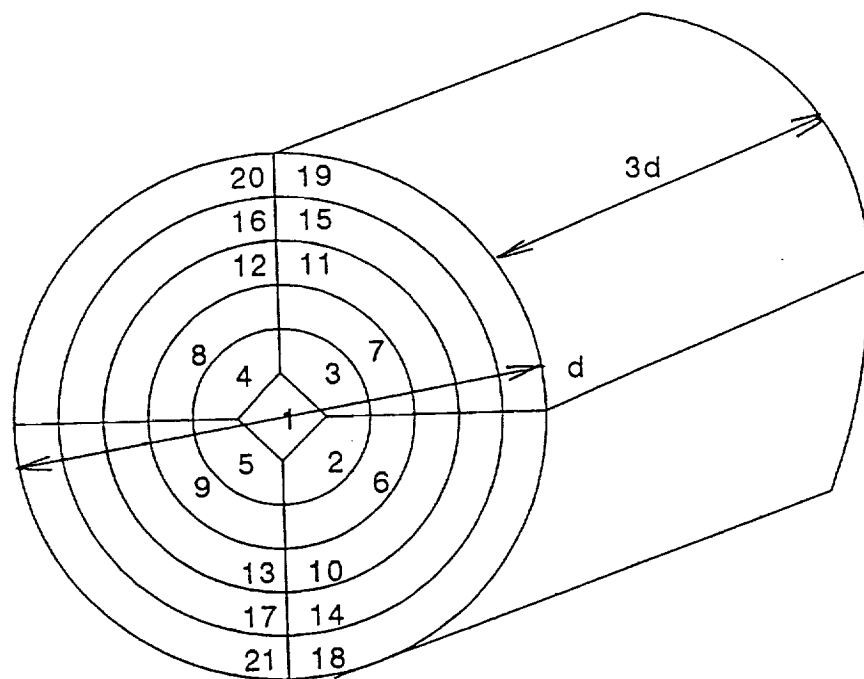


Fig.3 Finite Volume Element Structure

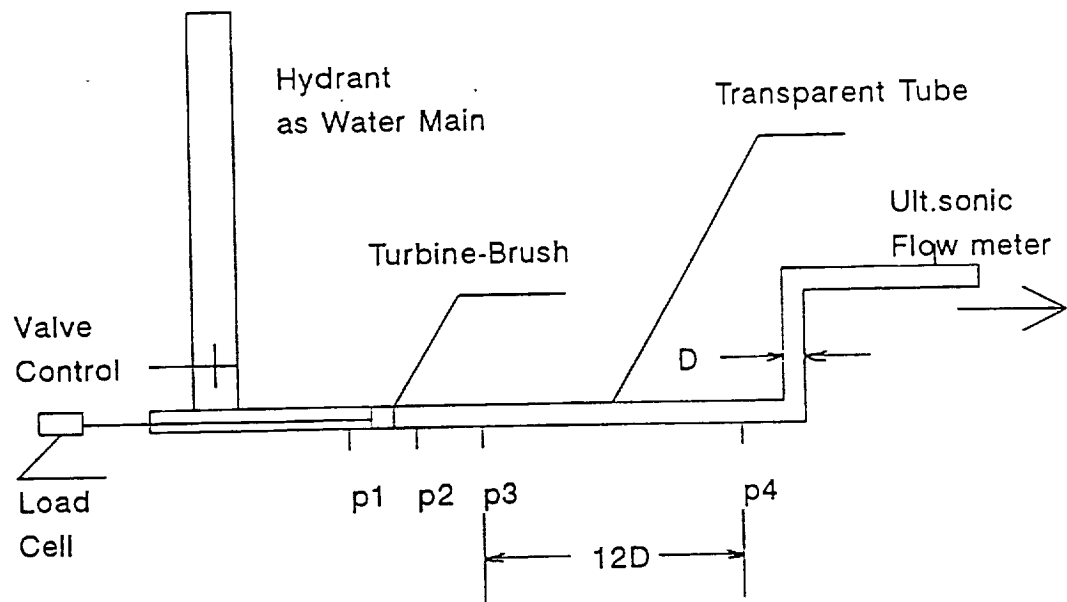
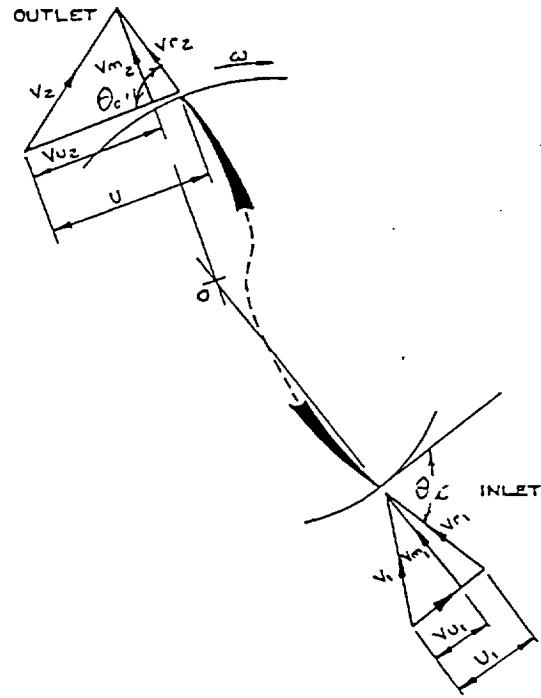
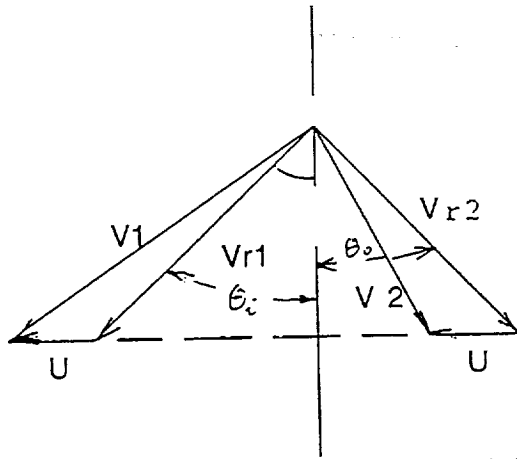


Fig.4 Experimental Apparatus and Probe Locations



(a) Inlet and Exit Vector Diagram



(b) Combined Vector Diagram at Inlet, Exit of a Blade of a Turbine

Fig.5 Inlet and Exit Vector Diagram and a Combined Vector Diagram

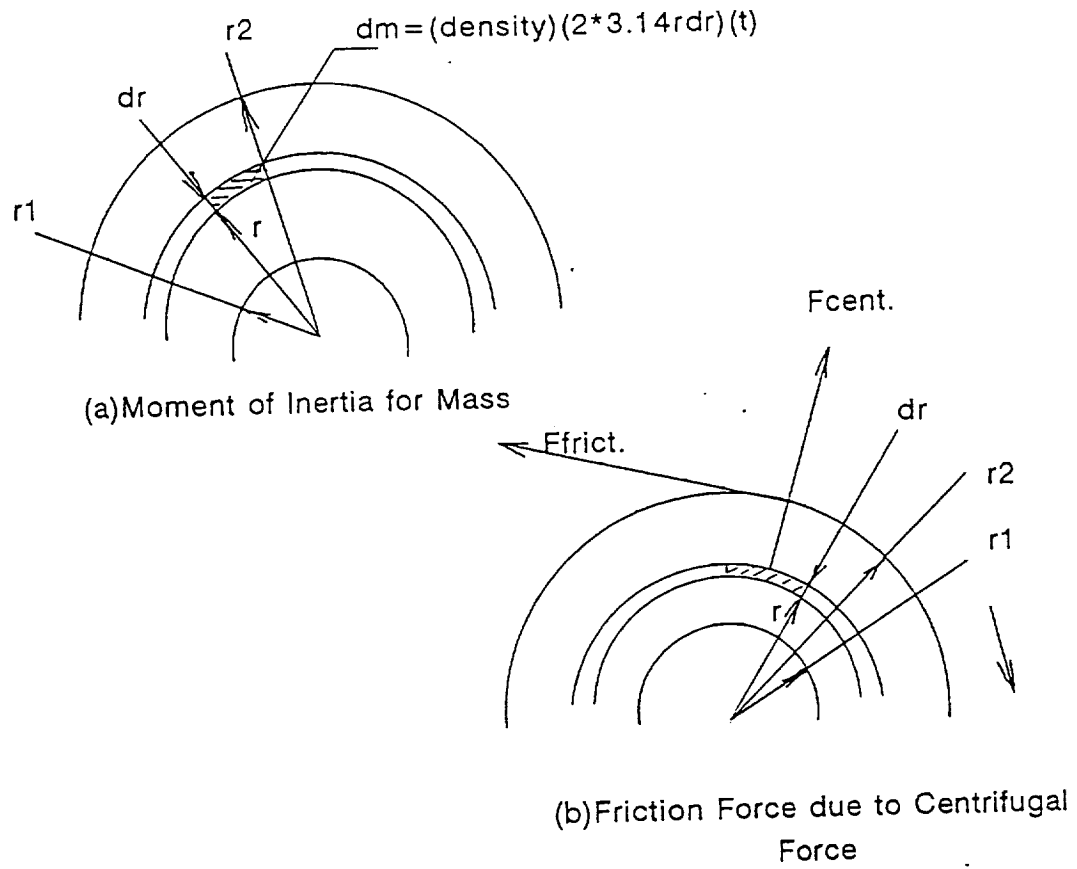


Fig.6 Mass Moment of Inertia, Centrifugal Force, Friction Force

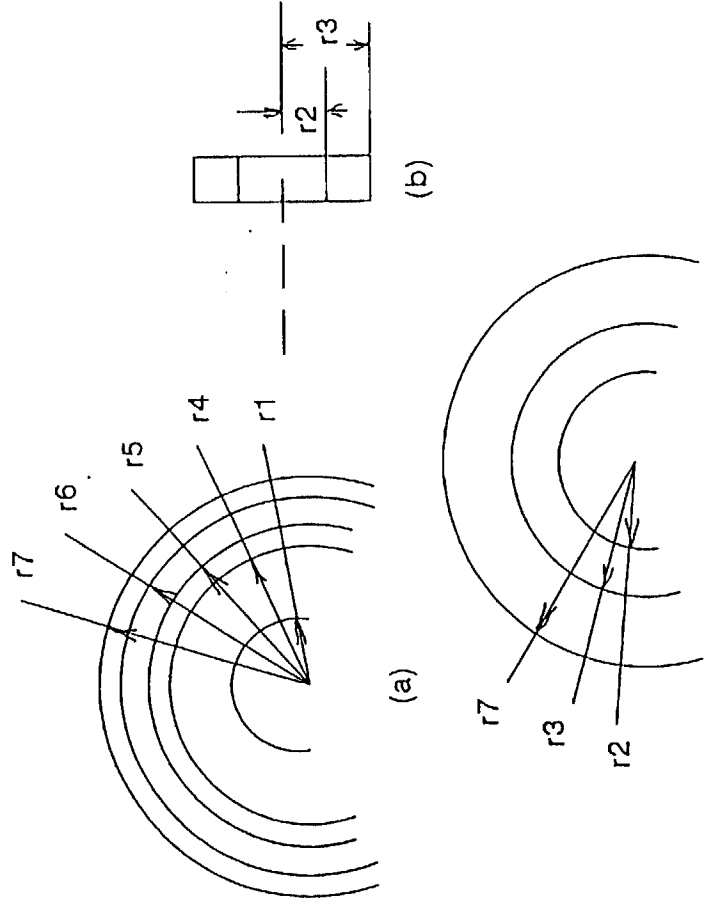


Fig.7 Radii of Turbine-Brush (a) Turbine and its Housing
 (b) Connector, (c) Brush